

## Vibration-Rotation Problem for Triatomic Molecules with Two Large-Amplitude Coordinates

### Spherical Model<sup>1</sup>

V. A. ISTOMIN, N. F. STEPANOV, AND B. I. ZHILINSKII

*Molecular Spectroscopy Laboratory, Department of Chemistry, Moscow State University  
Moscow, 117 234, USSR*

The vibration-rotation problem of a triatomic molecule composed of a rigid diatomic core and an atom which possesses almost free motion around this core is discussed. Such molecules as LiCN and KCN are appropriate examples. A model with two large-amplitude coordinates is used for calculations. Numerical results are presented using model potentials corresponding to the ab initio potential surface for the LiCN molecule.

#### I. INTRODUCTION

The theory of the vibration-rotation spectra of nonrigid molecules with one large-amplitude coordinate is now developed in detail (1-12). Besides this, group-theoretical techniques enable us to classify the vibration-rotation states of such nonrigid molecules (see review (13)). However, there are molecules for which more than one large-amplitude coordinate must be introduced (8).

Let us consider, for example, inorganic salts with ionic or partially ionic chemical bonds. Such molecules exhibit large-amplitude motion of the metal atom relative to the acid residue. Electron diffraction data for TlReO<sub>4</sub> (14) demonstrate the validity of a model according to which the motion of Tl is nearly spherical around the ReO<sub>4</sub> tetrahedron. Such molecules as M<sub>2</sub>SO<sub>4</sub>, MNO<sub>3</sub>, MCN, MBO<sub>2</sub>, etc. (M = alkali metal atom) possess similar properties. (See, for example, the recent review by Rambidi (15)). The van der Waals-type molecules X-A<sub>2</sub>, X-AB, X-ABC (X, inert gas atom; A<sub>2</sub>, AB, ABC, valence saturated molecules) provide other examples (12). All these molecules have a rigid core and an atom allowing for the large amplitude motion. To describe the low-frequency intramolecular motion in such systems it seems insufficient to use one large-amplitude coordinate. The problem becomes more complicated if the low-frequency motion is coupled with the core bending motions (16, 17).

In this paper we consider the simplest case of a molecule composed of an atom and a rigid diatomic core. An example of this kind of molecule is LiCN; Clementi *et al.* (18-19) have shown by ab initio calculations that the Li<sup>+</sup> ion in LiCN can move almost freely around the CN<sup>-</sup> group at the appropriate temperature.

<sup>1</sup> Presented at the Third All-Union Symposium on Molecular Spectroscopy of High and Super-high Resolution, Novosibirsk, September 1976.

A general approach was developed recently (20, 21) which permits the investigation of molecules with any number of nonrigid coordinates. Some theoretical publications have been devoted to triatomic nonrigid van der Waals molecules (12, 22, 23). But the explicit introduction of the body-fixed coordinate frame is not used in these works.

To calculate the vibration-rotation levels of a triatomic system with a diatomic rigid core, we suppose first the fulfillment of the adiabatic approximation then separate the center of mass of the system and introduce a body-fixed frame, connected only with the diatomic fragment. The location of the atom with respect to the diatomic core is characterized by two large-amplitude coordinates,  $r$ ,  $\theta$  (Fig. 1). An effective Hamiltonian is constructed to describe the motion of the atom around the core and the rotation of the molecule as a whole. The variational method is used to calculate the vibration-rotation energy levels and wavefunctions. In our treatment we follow the ideas of earlier works (3-5, 7, 9), and extend them to a more general scheme.

## II. INTERNAL COORDINATES AND HAMILTONIAN

The choice of the internal coordinates is presented in Fig. 1.  $\bar{r}_a$ ,  $\bar{r}_b$ ,  $\bar{r}_c$  are the position vectors of particles  $a$ ,  $b$ ,  $c$  in the space-fixed axis system. We define the relative coordinates  $\bar{R}$  and  $\bar{r}$  in such a way that the point 0 is arbitrarily placed on the  $\bar{R}$  vector. When atom  $c$  is chemically bound to atom  $a$  or  $b$  it is suitable to put the point 0 into coincidence with atom  $a$  or  $b$ , respectively. If atom  $c$ , in contrast, may be found in the neighborhood of atom  $a$  as well as  $b$ , to put the point 0 between  $a$  and  $b$  is more appropriate. Putting 0 at the center of mass of  $a$  and  $b$  results in the usual Jacobi coordinates for three particles. To specify the internal coordinates we use the body-fixed coordinate system with the  $z$  axis directed along the diatomic core. Then  $R$ ,  $r$ , and  $\theta$  are used as the internal coordinates. The core composed of atoms  $a$  and  $b$  is supposed to be rigid and thus  $R$  is a small-amplitude coordinate whereas  $r$  and  $\theta$  are two large-amplitude coordinates.

Under the adiabatic approximation the Hamiltonian may be written in Cartesian coordinates as

$$H = -\frac{1}{2m_a} \Delta_{\bar{r}_a} - \frac{1}{2m_b} \Delta_{\bar{r}_b} - \frac{1}{2m_c} \Delta_{\bar{r}_c} + V(|\bar{r}_i - \bar{r}_j|). \quad (1)$$

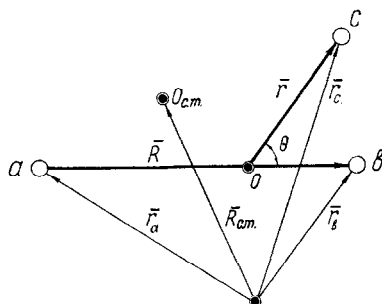


FIG. 1. Coordinates for three particles.

Introduce the vectors  $\vec{R}_{c.m.}$ ,  $\vec{R}$ ,  $\vec{r}$  (in analogy with (24))

$$\begin{aligned}\vec{R}_{c.m.} &= \frac{m_a \vec{r}_a + m_b \vec{r}_b + m_c \vec{r}_c}{m_a + m_b + m_c}, \\ \vec{R} &= \vec{r}_b - \vec{r}_a, \\ \vec{r} &= \vec{r}_c - \frac{\beta_a \vec{r}_a + \beta_b \vec{r}_b}{\beta_a + \beta_b}.\end{aligned}\quad (2)$$

Variation of  $\beta$  moves the point 0 along the  $\vec{R}$  vector. (For example, the choice  $\beta_a = m_a$ ;  $\beta_b = m_b$  put the point 0 into the center of mass of the rigid core.) Using coordinates (2) the Hamiltonian (1) may be rewritten as

$$H = -\frac{1}{2M} \Delta_{R_{c.m.}} - \frac{1}{2\mu_1} \left[ \Delta_{\vec{R}} + \frac{x}{2} (\nabla_{\vec{R}} \nabla_{\vec{r}} + \nabla_{\vec{r}} \nabla_{\vec{R}}) + \frac{x^2}{4} \Delta_{\vec{r}} \right] - \frac{1}{2\mu_2} \Delta_{\vec{r}} + V(\vec{r}, \vec{R}), \quad (3)$$

where

$$\begin{aligned}\frac{1}{\mu_1} &= \frac{1}{m_a} + \frac{1}{m_b}, & \frac{1}{\mu_2} &= \frac{1}{m_c} + \frac{1}{m_a + m_b}, \\ x &= \frac{m_b - m_a}{m_a + m_b} - \frac{\beta_b - \beta_a}{\beta_a + \beta_b}, \\ M &= m_a + m_b + m_c.\end{aligned}$$

Now we transform the Hamiltonian to the body-fixed coordinate system with the  $z$  axis directed along the diatomic core. Such a choice of coordinates was used earlier in the theory of diatomic molecules (25, 26) and in the three-particle problem (24). The body-fixed coordinate system is defined in the space-fixed coordinate frame by the Euler angles  $\alpha, \beta, \gamma$ , connected with the spherical coordinates of vectors  $\vec{R} = (R, \theta_1, \varphi_1)$  and  $\vec{r} = (r, \theta_2, \varphi_2)$  by relations  $\alpha = \varphi_1, \beta = \theta_1, \gamma = 0$ .

$$\begin{aligned}H &= -\frac{1}{2\mu_1} \left[ \frac{\partial^2}{\partial R^2} + \frac{2}{R} \frac{\partial}{\partial R} + \frac{x^2}{4} \Delta_{\vec{r}} \right] - \frac{1}{2\mu_2} \Delta_{\vec{r}} \\ &+ \frac{1}{2\mu_1 R^2} [J^2 + L^2 - (2L_z^2 + L_+ J_- + L_- J_+)] \\ &- \frac{x}{8\mu_1 R} [L_+ P_- + L_- P_+ + P_+ L_- + P_- L_+] \\ &+ \frac{x}{4\mu_1 R} [P_+ J_- + P_- J_+] - \frac{x}{4\mu_1} \left[ \frac{\partial}{\partial R} \frac{\partial}{\partial z} + \frac{\partial}{\partial z} \frac{\partial}{\partial R} + \frac{2}{R} \frac{\partial}{\partial z} \right] + V(R, r, \theta). \quad (4)\end{aligned}$$

Here

$$L_{\pm} = L_x \pm iL_y,$$

and  $L_x, L_y, L_z$  are components of the angular momentum operator for particle associated with vector  $\bar{r}$ ,  $P$  is a momentum operator for the particle associated with vector  $\bar{r}$ . The operators  $L$  and  $P$  are identified in the body-fixed system  $x, y, z$ .

$J$  is the total orbital angular momentum for the three-particle problem. The definition and the explicit expressions of the  $J_{\pm}$  operators in terms of angular variables are represented in Appendix 1. The rules for  $J_{\pm}$  acting on generalized spherical functions are listed there as well.

The terms including  $P_{\pm}$  and  $\partial/\partial z$  operators correspond to mass polarization corrections in the theory of diatomic molecules. They vanish under the  $x = 0$  coordinate choice. In such a case there are no cross terms involving the products of the differential operators with respect to the rigid coordinate  $R$  and the angular variables. The Hamiltonian (4) is suitable in this sense for the approximate separation of the rigid ( $R$ ) coordinate.

To construct the effective nonrigid Hamiltonian with two internal degrees of freedom we average the Hamiltonian (4) with the vibrational harmonic function depending on  $R$ . The resulting Hamiltonian depends on  $r$  and  $\theta$  as well as on the external variables  $\theta_1, \varphi_1, \varphi$

$$H = - \left( \frac{x^2}{8\mu_1} + \frac{1}{2\mu_2} \right) \Delta_{\bar{r}} + \frac{1}{2\mu_1 R_0^2} (J^2 + L^2) - \frac{1}{2\mu_1 R_0^2} (2L_z^2 + L_+ J_- + L_- J_+) - \frac{x}{8\mu_1 R_0} [P_+ L_- + P_- L_+ + L_- P_+ + L_+ P_- - 2(P_+ J_- + P_- J_+)] + V(r, \theta). \quad (5)$$

$V(r, \theta)$  is the potential integrated over the  $R$ -dependent vibrational function.  $R_0$  is some effective value of  $R$ . A more accurate treatment should use the second-order perturbation theory in analogy with the work of Hoy and Bunker (5). But here we use the simple form (5) and consider the evaluation of eigenvalues and eigenfunctions of operator (5). For this purpose auxiliary Hamiltonians will be constructed with the help of the subdivision of operator (5). Certainly the representation of potential energy in spherical coordinates is not suitable for highly elliptical potential surfaces due to the bad separation of variables. The preliminary scaling may be useful to obtain coordinates more suited for the potential representation and on the other hand to yield a rather simple form of kinetic energy. The resulting elliptical model will be discussed in a later work.

### III. VARIATIONAL TECHNIQUE

In order to avoid the two-dimensional numerical integration we use the special form of potential expansion which is suitable for the problem considered:

$$V = \sum_{k,m} C_{km} (r - r_0)^k \cos^m \theta, \quad (6)$$

where  $r_0$  is some averaged value of  $r$ .

Then we employ the variational procedure. We construct the basis by preliminary crude separation of variables in the Hamiltonian (5). For the sake of simplicity we put  $x = 0$  which means that the point 0 coincides with the center of mass of the rigid core.

(The bending Hamiltonian for  $x \neq 0$  will be discussed in Appendix 2.) On the first step we introduce two Hamiltonians  $H_r$  and  $H_\theta$ :

$$H_r = -\frac{1}{2\mu_2 r^2} \frac{\partial}{\partial r} \left( r^2 \frac{\partial}{\partial r} \right) + V_r(r); \quad (7)$$

$$H_\theta = \frac{1}{2\mu_1 R^2_0} J^2 + \left( \frac{1}{2\mu_1 R^2_0} + \frac{1}{2\mu_2 r^2_0} \right) L^2 - \frac{1}{2\mu_1 R^2_0} [2L^2_z + L_+ J_- + L_- J_+] + V_\theta(\theta). \quad (8)$$

The motion over the  $r$  variable is supposed to be close to  $r_0$ , and  $V_r(r)$  as well as  $V_\theta(\theta)$  are effective potentials obtained in some way from the total potential (6). For example,

$$V_r(r) = \sum_{k=0} C_{k0} (r - r_0)^k, \quad (9)$$

$$V_\theta(\theta) = \sum_{m=0} C_{0m} \cos^m \theta.$$

If the radial motion is significantly more rigid than the angular one, the effective angular nonrigid Hamiltonian should be constructed from the operator (5) through averaging over the  $r$ -dependent function or even through the second-order perturbation theory.

Consider now the calculation of the eigenvalues and eigenfunctions of operators (7) and (8). The following functions are appropriate as basis functions for operator (7):

- (i) Radial eigenfunctions  $R_{n,l}$  of the three-dimensional harmonic oscillator.
- (ii) Eigenfunctions of the operator

$$H_{\text{osc}} = -\frac{1}{2\mu_2 r^2} \frac{\partial}{\partial r} \left( r^2 \frac{\partial}{\partial r} \right) + \frac{\mu_2 w^2}{2} (r - r_0)^2.$$

( $w$  is a variational parameter.) This operator possesses no analytical eigenfunctions. An approximate solution may be obtained by increasing the integration range from  $(0, \infty)$  to  $(-\infty, \infty)$ , supposing  $r_0$  is sufficiently far from zero.

- (iii) Radial eigenfunctions of the operator

$$H = - (1/2\mu_2) \Delta_{\bar{r}} - 2D[(a/r) - \frac{1}{2}(a^2/r^2)],$$

which have proved to be useful as zero-order functions for the vibrational problem (27).

Basis (ii) enables us to perform the matrix element calculation in the most simple way.

The operator (8) is natural to diagonalize in the basis

$$|l, k\rangle = \frac{1}{2^{\frac{1}{2}}} [D^J_{k0}(\varphi_1, \theta_1, 0) Y_{lk}(\theta, \varphi) \pm D_{-k0}(\varphi_1, \theta_1, 0) Y_{l,-k}(\theta, \varphi)], \quad (10)$$

$$|l, 0\rangle = D^J_{00} Y_{l0},$$

where  $D^J_{km}$  are the Wigner functions,  $Y_{lk}$  are spherical harmonics,  $J$  is the quantum number of the total angular momentum,  $k = 0, \dots, J$ . Unfortunately, large values of  $J$  require too large a basis. In such a case another method of solving the eigenvalue problem may be used which is briefly discussed in Appendix 3.

The multiplication of eigenfunctions of operators (7) and (8) leads to the basis for the calculation of the eigenvalues of operator (5). This basis gives the possibility of analytical evaluation of all matrix elements except  $\langle R_{n'} | 1/r^2 | R_n \rangle_r$  ones, which may be evaluated analytically only after the expansion of  $r^{-2}$  near the value  $r_0$ .

Some other methods of finding the eigenvalues of Hamiltonian (5) are considered in Appendix 3.

#### IV. COMPUTER PROGRAM

In the preceding section we proposed the algorithm which does not require numerical integration schemes. Here we briefly describe a computer program based on it. The program uses radial harmonic oscillator functions to find the eigenfunctions of  $H_r$ . No more than 60 functions may be used. Operator  $H_\theta$  is diagonalized in the basis of functions (10) and up to 100 functions may be used. The potential  $V(r, \theta)$  is taken as expansion (6) with  $0 \leq k \leq 4$ ,  $0 \leq m \leq 4$ . Hence  $V(r, \theta)$  depends maximally on 25 coefficients  $c_{km}$ . Potentials  $V_r(r)$  and  $V_\theta(\theta)$  are constructed from  $V(r, \theta)$  by formula (9). Besides, the effective potential  $V$  may be obtained in terms of the second-order perturbation theory by using eigenfunctions of  $H_r$ . Such a procedure is necessary when the cross coefficients  $c_{km}$  in the potential expansion are rather large.

The total basis may include up to 15 eigenfunctions of  $H_r$  and 20 eigenfunctions of  $H_\theta$ , with the total number of basis functions not exceeding 120. The program permits the calculation of the vibration-rotation energies up to  $J = 8$  ( $J_z = 0$ ). But results for high  $J$  values are good only for such favorable cases as the  $\text{ArO}_2$  molecule where the nearly free rotation of the Ar atom around the  $\text{O}_2$  core takes place. As we noted earlier the other algorithms are more suitable for the calculation of states with high  $J$  values.

#### V. RESULTS AND DISCUSSION

The program described above was used for vibration-rotation level calculations of the LiCN and KCN molecules with model potential of the form

$$V(r, \theta) = k_r(r - r_0)^2 + k_\theta(1 - \cos\theta). \quad (11)$$

The choice of the model potential is based on the known experimental and theoretical results on MCN-type molecules. The potential surface for the LiCN molecule was studied in (18, 19). The linear configurations of LiCN and LiNC were investigated more carefully. The LiNC configuration was shown to be more stable ( $0.3 \text{ eV} \approx 2420 \text{ cm}^{-1}$  lower than the LiCN one). Such a low barrier results in hindered rotation of the Li around the CN group at temperatures of about 1000 K. This indicates clearly that the LiNC molecule may be regarded as linear only for several lowest bending states.

Ismail *et al.* (30, 31) have studied the ir spectra of LiNC, NaCN, and KCN molecules incorporated into the inert gas matrix. The bending frequency of LiNC was found to be equal to  $119 \text{ cm}^{-1}$  (Ne matrix).

Recently the microwave spectrum for the KCN molecule was detected for  $J: 8 \rightarrow 9$ ;  $9 \rightarrow 10$ , and  $10 \rightarrow 11$  transitions at a temperature of about 600 K (32). The authors could not interpret the data obtained in terms of a linear KCN molecule, so they believed that the motion of K around the CN fragment takes place.

All these results suggest that the numerical investigation of the triatomic problem with the potential (11) would be interesting. We note that the model proposed is rather crude to yield quantitative agreement with the known experimental and theoretical results because the potential (11) reproduces the barrier height rather than the shape of the potential function. Nevertheless we hope that our results are interesting from the qualitative point of view.

Calculations for the LiCN molecule were performed with the following parameter values:  $r_0 = 4.36$  a.u.,  $k_r = 5 \times 10^{-2}$  a.u., and  $k_\theta = 1 \times 10^{-3}, 3.5 \times 10^{-3}, 5.5 \times 10^{-3}$  a.u. Results are obtained for  $J = 0-4$ . The C-N distance is equal to 2.19 a.u. (ab initio calculations of the potential surface were performed for LiNC nonlinear configurations at this internuclear distance). The value of the force constant  $k_r = 5 \times 10^{-2}$  a.u. corresponds to the frequency of the radial motion,  $\omega_r = 692.20$   $\text{cm}^{-1}$ . (More accurate treatment of Clementi's data (19) for linear configuration leads to  $\omega_r \approx 720-740$   $\text{cm}^{-1}$ .) The  $r_0$  value is also taken from the linear configuration LiNC. The bending force constant  $k_\theta = 5.5 \times 10^{-3}$  a.u. results in the same barrier as the ab initio calculations.

TABLE I  
Energy levels ( $\text{cm}^{-1}$ ) of radial-bending-rotation Hamiltonian  
( $J=0$ ) for LiNC model<sup>a</sup>

$V_1$	(N,L)	$V_2$	(N,L)	$V_3$	(N,L)
378.075	0,0	407.033	0,0	422.806	0,0
441.944	0,1	528.858	0,1	576.185	0,1
503.033	0,2	648.036	0,2	726.942	0,2
561.113	0,3	764.471	0,3	875.006	0,3
615.881	0,4	878.056	0,4	1020.297	0,4
666.890	0,5	988.667	0,5	1115.049	1,0
713.441	0,6	1096.163	0,6	1162.728	0,5
753.952	0,7	1099.266	1,0	1268.513	1,1
787.167	0,8	1200.376	0,7	1302.200	0,6
822.099	0,9	1221.160	1,1	1419.354	1,2
865.851	0,10	1301.105	0,8	1438.606	0,7
916.911	0,11	1340.402	1,2	1567.498	1,3
1037.290	0,12	1398.106	0,9	1571.820	0,8
1070.563	1,0	1456.899	1,3	1701.702	0,9
1105.924	0,13	1491.067	0,10	1712.866	1,4
1134.101	1,1	1570.542	1,4	1807.291	2,0

<sup>a</sup>Triaxial potentials:  $V_1 = 5.0 \times 10^{-2} (r - r_0)^2 + k_1 (1 - \cos \theta)$  a.u.,  
 $k_1 = 1 \times 10^{-3}$ ,  $k_2 = 3.5 \times 10^{-3}$ ,  $k_3 = 5.5 \times 10^{-3}$ ,  $r_0 = 4.36$  a.u.,  
 N,L, - radial, bending quantum numbers.

TABLE II  
Energy levels ( $\text{cm}^{-1}$ ) of radial-bending-rotation Hamiltonian for LiNC model<sup>a</sup>.

$J = 0$	(N,L)	$J = 1-$	(N,L)	$J = 1+$	(N,L)	$J = 2-$	(N,L)	$J = 2+$	(N,L)
422.806	0,0	500.787	0,0	423.699	0,0	502.594	0,0	425.485	0,0
576.185	0,1	652.890	0,1	500.777	0,1	579.173	0,1	502.563	0,1
726.942	0,2	802.339	0,2	577.088	0,2	654.732	0,2	578.909	0,2
875.006	0,3	949.060	0,3	652.868	0,3	730.004	0,3	579.178	0,3
1020.297	0,4	1092.969	0,4	727.858	0,4	804.219	0,4	654.768	0,4
1115.049	1,0	1193.074	1,0	802.304	0,5	878.150	0,5	730.050	0,5
1162.728	0,5	1233.975	0,5	875.935	0,6	950.983	0,6	730.242	0,6

<sup>a</sup> $V(x, \theta) = 5.0 \times 10^{-2}(x-r_0)^2 + 5.5 \times 10^{-3}(1-\cos\theta)$  a.u. ;  $r_0 = 4.36$  a.u. ; radial frequency -  $692.2 \text{ cm}^{-1}$ . (N,L) - radial, bending quantum numbers.

In the KCN calculations  $k_\theta = 5.0 \times 10^{-3}$  and  $4.0 \times 10^{-3}$  a.u. The geometrical parameters for the KCN molecule are:  $r_0 = 2.57 \text{ \AA}$ ,  $R(\text{CN}) = 1.15 \text{ \AA}$  (31). The influence of the basis size on the accuracy is discussed in Appendix 4.

Energy levels for some model potentials are listed in Tables I and II. Figure 2 represents for the sake of clarity the energy levels of the bending-rotation Hamiltonian  $H_\theta$  for  $J = 0$ . The distribution of low levels corresponds to the anharmonic oscillator model. The level separation becomes smaller at the top of the barrier. Above the top the arrangement of the levels resembles the free rotator one. The same behavior was earlier observed for the quasi-linear molecules. The correlation between free rotation and re-

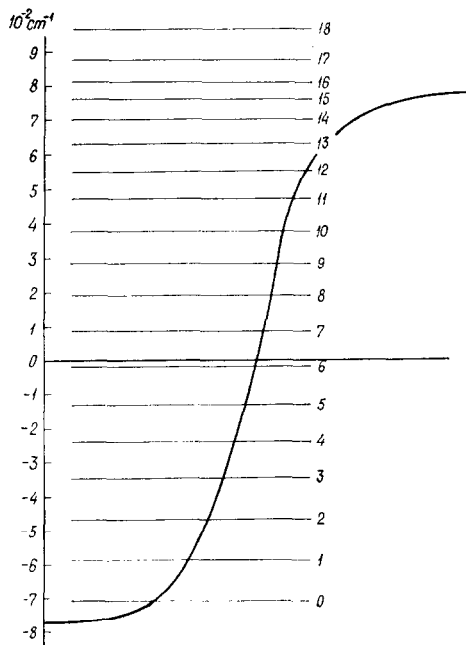


FIG. 2. Bending states for the LiNC molecule.  $V(\theta) = -3.5 \times 10^{-3} \cos\theta$  a.u.



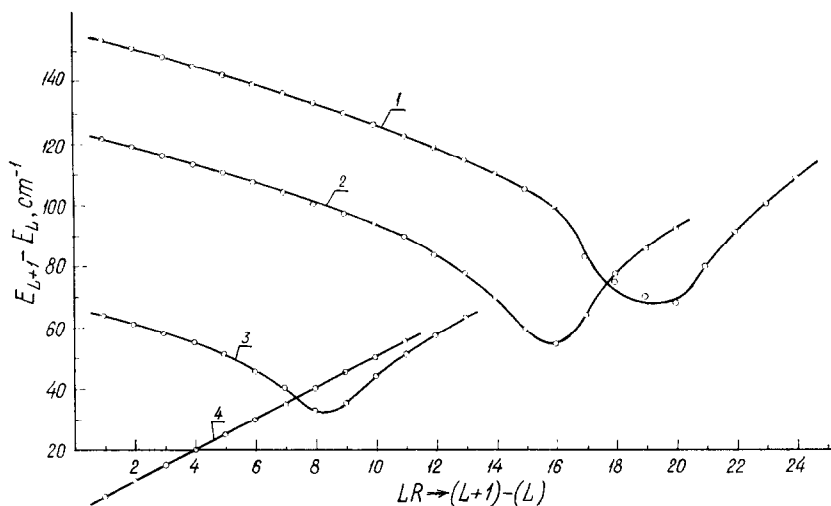


FIG. 3. Frequencies of the  $L \rightarrow L + 1$  transitions (numbered as  $LR$ ) in the LiNC molecule for model potentials  $V(\theta)$ .  $L$ , quantum number for  $H_\theta$  Hamiltonian,  $J = 0$ . 1 -  $V(\theta) = -5.5 \times 10^{-3} \cos\theta$  a.u.; 2 -  $V(\theta) = -3.5 \times 10^{-3} \cos\theta$  a.u.; 3 -  $V(\theta) = -1.0 \times 10^{-3} \cos\theta$  a.u.; 4 -  $V(\theta) = 0$ .

stricted rotation levels permits correlation of the quantum numbers  $v, l'$  of the two-dimensional isotropic harmonic oscillator with the free rotator quantum numbers. A similar correlation can be obtained for levels which differ significantly from the linear molecule levels. The effect of the high level density at the top of the barrier is shown in Fig. 3. The frequencies of the  $L \rightarrow L + 1$  transitions are presented there for three different potentials ( $L$  denotes the quantum number of Hamiltonian  $H_\theta$ ). The  $L$  dependence is linear for low levels. The minimum takes place at the top of the barrier and above the barrier all curves go to their asymptotic values corresponding to the linear change of the frequency for the free rotator. The analogous frequency dependence is shown in Fig. 4 for the KCN molecule.

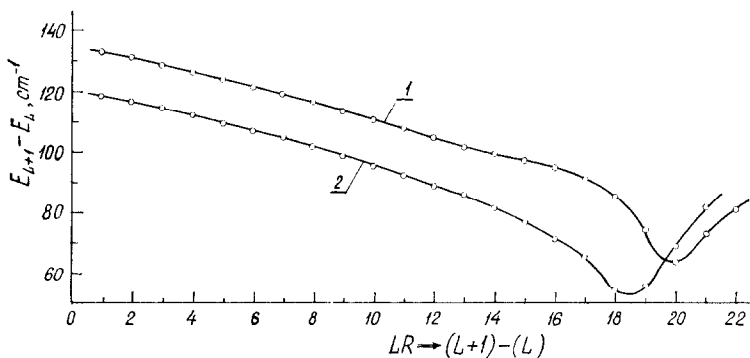


FIG. 4. Frequencies for the  $L \rightarrow L + 1$  transitions in the KCN molecule for model potentials  $V(\theta)$ .  $L$ , quantum number for  $H_\theta$  Hamiltonian,  $J = 0$ . 1 -  $V(\theta) = -5.0 \times 10^{-3} \cos\theta$  a.u.; 2 -  $V(\theta) = -4.0 \times 10^{-3} \cos\theta$  a.u.

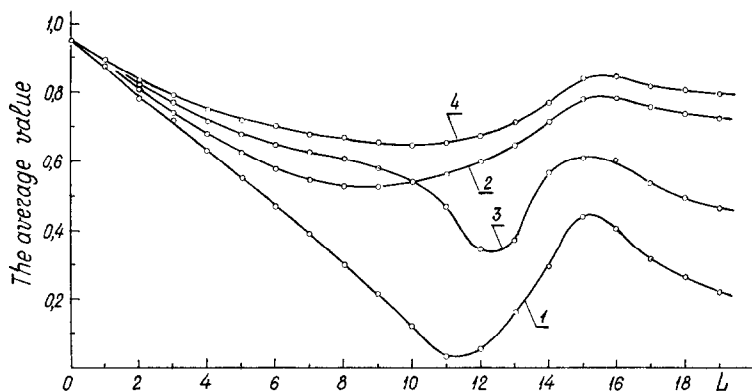


FIG. 5. Average values of  $\cos^n \theta$  for the LiNC model Hamiltonian  $H$ , ( $J = 0$ ),  $V(\theta) = -3.5 \times 10^{-3} \cos \theta$  a.u. 1 —  $|\langle L |\cos \theta| L \rangle|$ ; 2 —  $\langle L |\cos^2 \theta| L \rangle$ ; 3 —  $|\langle L |\cos^3 \theta| L \rangle|$ ; 4 —  $\langle L |\cos^4 \theta| L \rangle$ .

Average values of  $\cos^n \theta$ ,  $n = 1-4$ , at  $J = 0$  are calculated along with the energy characteristics. These values are presented in Fig. 5 for one of the trial potentials as functions of the quantum number for the bending Hamiltonian. The change of  $\langle \cos \theta \rangle$  with increasing barrier height is shown in Fig. 6. The value  $\theta = 0$  corresponds to the linear configuration LiNC. As the barrier exists for the LiCN linear configuration,  $\langle \cos \theta \rangle$  is close to 1 for low bending levels and decreases with excitation of the bending vibration. For the levels at the barrier top the average value of  $\cos \theta$  becomes negative. This may be explained by the fact that for this energy the turning points are in the angle region  $\theta > \pi/2$ . The wavefunctions for the levels lying above the barrier closely resemble the  $Y_{10}$  ones. So the average value of  $\cos \theta$  goes to zero. The analogous dependence of the average value of  $\cos \theta$  is shown in Fig. 7 for the KCN molecule.

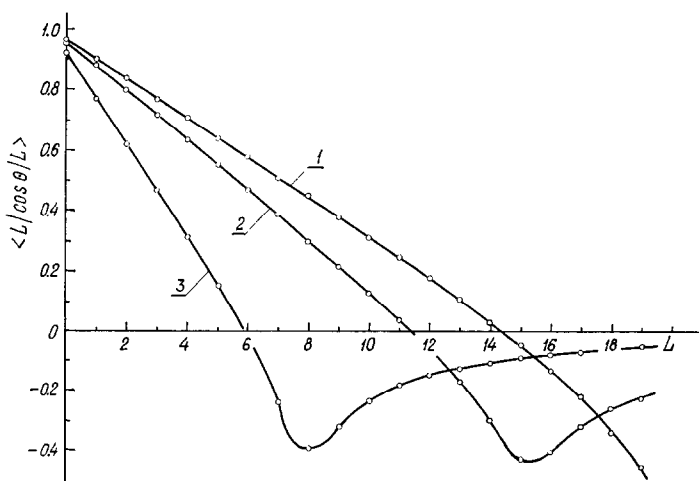


FIG. 6. The average value of  $\cos \theta$  for the LiNC model Hamiltonian ( $J = 0$ ). 1 —  $V(\theta) = -5.5 \times 10^{-3} \cos \theta$  a.u.; 2 —  $V(\theta) = -3.5 \times 10^{-3} \cos \theta$  a.u.; 3 —  $V(\theta) = -1.0 \times 10^{-3} \cos \theta$  a.u.

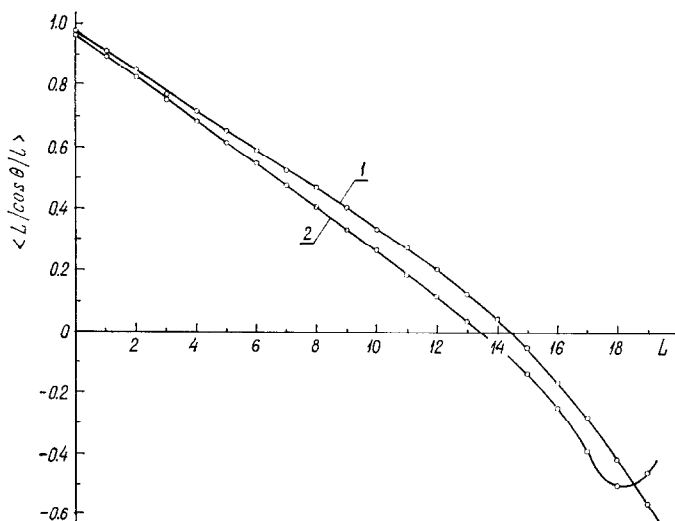


FIG. 7. The average value of  $\cos\theta$  for the KCN model Hamiltonian ( $J = 0$ ). 1 -  $V(\theta) = -5.0 \times 10^{-3} \cos\theta$  a.u.; 2 -  $V(\theta) = -4.0 \times 10^{-3} \cos\theta$  a.u.

The average values presented in Figs. 5-7 are calculated for  $J = 0$ . But they do not practically change under  $J$  variation, especially for low vibrational levels.

The effective rotational constants  $B_v$  and  $D_v$  may be introduced regarding LiNC as linear molecule. The  $B_v$  and  $D_v$  dependence on quantum number  $v$  for the bending Hamiltonian is of primary interest in view of the preliminary results of the microwave spectrum of KCN for which the anomalous  $D_v$  dependence was obtained (32).

Figure 8 shows the  $J(0 \rightarrow 1)$  dependence for the bending Hamiltonian with some trial potentials. The ordinary linear molecules demonstrate a linear  $J(0 \rightarrow 1)$  dependence. As it follows from Fig. 8, even the first levels of the LiCN model with the potential  $V(\theta) = -1.0 \times 10^{-3} \cos\theta$  do not lie on a straight line. The barrier for this molecule is significantly higher for the ab initio potential. Nevertheless the  $J(0 \rightarrow 1)$  transition has a well-defined parabolic dependence for low-lying levels. Using the  $J = 0, 1, 2$  energy levels enables us to construct the  $B_v$  and  $D_v$  dependences. We suppose that the relation

$$E_v = B_v J(J+1) - D_v J^2(J+1)^2$$

is valid for  $l' = 0$  ( $l'$  is the quantum number of the vibrational angular momentum for the two-dimensional harmonic oscillator) and introduce

$$E_v^1 = E_{J=1,v} - E_{J=0,v}; \quad E_v^2 = E_{J=2,v} - E_{J=0,v}.$$

Then

$$B_v = (9E_v^1 - E_v^2)/12; \quad D_v = (3E_v^1 - E_v^2)/24.$$

The dependences obtained in this way are represented in Fig. 9. The anomalous  $D_v$  dependence is obvious. Unfortunately we cannot obtain the  $D_v$  and  $B_v$  dependences taking into account the  $J = 0, 1, 2, 3, \dots$  levels. The reliability of level positions with simultaneously high  $J$  and  $v$  values is insufficient for such purposes. (We believe an accuracy of about  $0.001 \text{ cm}^{-1}$  would be needed.)

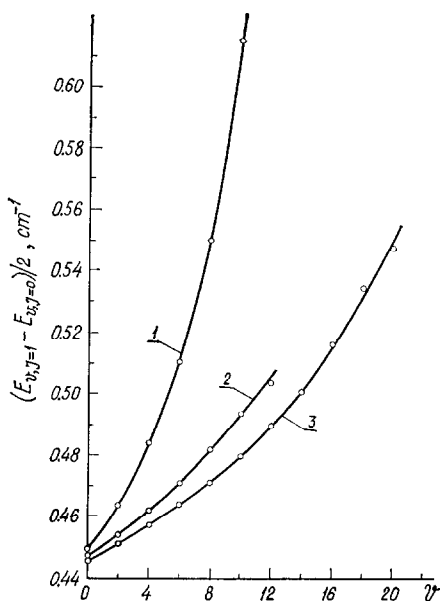


FIG. 8. Dependence of the  $J = 1-0$  transition on quantum number  $v$  for the LiNC molecule. 1 —  $V(\theta) = -1.0 \times 10^{-3} \cos\theta$  a.u.; 2 —  $V(\theta) = -3.5 \times 10^{-3} \cos\theta$  a.u.; 3 —  $V(\theta) = -5.5 \times 10^{-3} \cos\theta$  a.u.

Figure 10 shows the frequencies of the  $L \rightarrow L + 1$  transitions for the bending rotation Hamiltonian for a different choice of internal coordinates (the case with  $x \neq 0$ ). The corresponding Hamiltonian is presented in Appendix 2.

Until now we considered the  $H_\theta$  Hamiltonian. The diagonalization of the  $H$  operator results in the bending-rotation structure of each radial vibrational level. The bending frequencies do not significantly change under the excitation of radial levels (see Table II). This is connected with the absence of terms responsible for radial-bending inter-

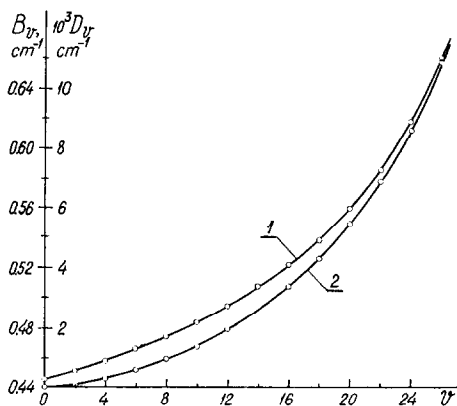


FIG. 9.  $B_v$  and  $D_v$  dependence on the quantum number  $v$  for the LiNC molecule.  $V(\theta) = -5.5 \times 10^{-3} \cos\theta$  a.u.; 1 —  $B_v$ ; 2 —  $D_v$ .

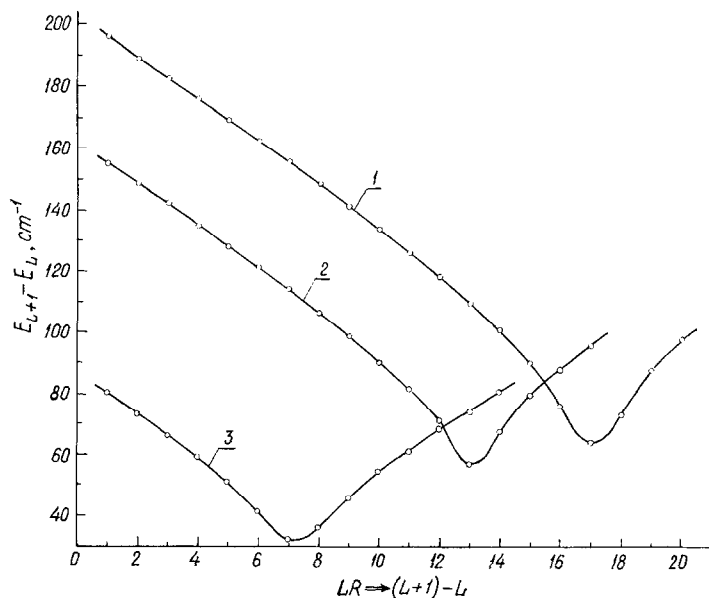


FIG. 10. Frequencies of the  $L \rightarrow L + 1$  transitions in the LiNC molecule for model potentials  $V(\theta)$  with special choice of coordinates ( $x \neq 0$ ).  $r_0 = 3.349$  a.u.; 1 -  $V(\theta) = -5.5 \times 10^{-3} \cos\theta$  a.u.; 2 -  $V(\theta) = -3.5 \times 10^{-3} \cos\theta$  a.u.; 3 -  $V(\theta) = -1.0 \times 10^{-3} \cos\theta$  a.u.;  $r$  is the internuclear distance N-Li.

action in the potential. Such terms arise when the elliptical character of the Li motion is introduced. Here the centrifugal distortion is only taken into account in the total Hamiltonian. But it is relatively small due to the high frequency of the radial vibrations.

One should mention that the frequency  $\nu_2 = 78\text{--}98$   $\text{cm}^{-1}$  was obtained for the model potentials which reproduce the *ab initio* barrier. These results are not in good agreement with the value of Ismail *et al.* (30),  $\nu_2 = 119$   $\text{cm}^{-1}$ . Two sources of errors may be responsible for this discrepancy: the neglect of the elliptical character of the Li motion and the difficulty in obtaining proper quantitative information about the potential surface for the Li motion from the data of Clementi *et al.* In particular, the recalculation of the LiCN potential surface for nonlinear configurations would be desirable.

In concluding this section we note that the main idea of our calculations was to clarify the qualitative regularities in the vibration-rotation spectra of specific nonrigid molecules.

## CONCLUSIONS

The results presented here are the first ones obtained with our program for ionic molecules. We intend to apply the model to the interpretation of the microwave spectra of the KCN molecule. At the same time this technique can be used for the calculation of vibration-rotation spectra of van der Waals complexes. The more detailed information on this investigation will be published elsewhere. Further theoretical extension of our work will concern more complex molecules consisting of a rigid core and one atom

performing a large-amplitude motion around this core (for example, a  $\text{LiBH}_4$  molecule), however, the specific type of molecule would depend mainly upon the experimental data for the gaseous molecules which are now available.

## APPENDIX 1

The explicit expressions for the  $J^2$ ,  $J_{\pm}$ ,  $P_{\pm}$  operators are listed here, as well as the rules of their actions on basic functions:

$$J^2 = - \left[ \frac{1}{\sin\theta_1} \frac{\partial}{\partial\theta_1} \sin\theta_1 \frac{\partial}{\partial\theta_1} + \left( \frac{1}{\sin\theta_1} \frac{\partial}{\partial\varphi_1} - iL_z \text{ctg}\theta_1 \right)^2 \right] + L_z^2,$$

$$J_{\pm} = \pm \frac{\partial}{\partial\theta_1} + \frac{i}{\sin\theta_1} \frac{\partial}{\partial\varphi_1} + L_z \text{ctg}\theta_1,$$

$$J_z = L_z = -i \frac{\partial}{\partial\varphi},$$

$$L^2 = - \left[ \frac{1}{\sin\theta} \frac{\partial}{\partial\theta} \sin\theta \frac{\partial}{\partial\theta} + \frac{1}{\sin^2\theta} \frac{\partial^2}{\partial\varphi^2} \right],$$

$$L_{\pm} = e^{\pm i\varphi} \left[ \pm \frac{\partial}{\partial\theta} + i \text{ctg}\theta \frac{\partial}{\partial\varphi} \right],$$

$$P_z = i \left[ \cos\theta \frac{\partial}{\partial r} - \frac{\sin\theta}{r} \frac{\partial}{\partial\theta} \right],$$

$$\begin{aligned} P_{\pm} &= \pm iP_x - P_y \\ &= e^{\pm i\varphi} \left( \pm \sin\theta \frac{\partial}{\partial r} + \frac{\cos\theta}{r} \frac{\partial}{\partial\theta} + i \frac{1}{r \sin\theta} \frac{\partial}{\partial\varphi} \right). \end{aligned}$$

The generalized spherical functions  $D^J_{MK}(\varphi_1, \theta_1, 0)$  are defined as in Ref. (33), but they are normalized to unity with respect to two angles  $\varphi_1$  and  $\theta_1$ . The rules for the action of  $J^2$ ,  $J_{\pm}$  upon  $D^J_{MK}$  as well as  $L_z$ ,  $P_{\pm}$ ,  $P_z$  upon  $Y_{lk}$  are sufficient for the problem considered:

$$J^2 D^J_{MK} = J(J+1) D^J_{MK},$$

$$J_{\pm} \chi(\varphi_1, \theta_1) \frac{e^{im\varphi}}{(2\pi)^{\frac{1}{2}}} = [J_{\pm}(m) \chi(\varphi_1, \theta_1)] \frac{e^{im\varphi}}{(2\pi)^{\frac{1}{2}}},$$

where  $\chi(\varphi_1, \theta_1)$  is an arbitrary function of  $\varphi_1$  and  $\theta_1$

$$J_{\pm}(M) = \pm \frac{\partial}{\partial\theta_1} + \frac{i}{\sin\theta} \frac{\partial}{\partial\varphi_1} + M \text{ctg}\theta_1,$$

$$J_{\pm}(M) D^J_{MK}(\varphi_1, \theta_1, 0) = [J(J+1) - M(M \pm 1)]^{\frac{1}{2}} D^J_{M \pm 1, K}.$$

The physical meaning of  $J_{\pm}(M)$  operators was discussed recently by Hougen (34, 35).

The rules of  $P_{\pm}$ ,  $P_z$  acting on  $Y_{lm}$  may easily be obtained from the well-known relations for  $Y_{lm}$  (36).

## APPENDIX 2

We use the change of variables which removes the weight factor and results in  $\partial/\partial r \rightarrow (\partial/\partial r) - (1/r)$ . To obtain the  $H_{\theta}$  operator for  $x \neq 0$  we introduce operators

$$P^{(\theta)}_{\pm} = \pm \frac{e^{\pm i\varphi}}{r_0} \left[ \cos\theta \frac{\partial}{\partial \theta} - \sin\theta \right] - \frac{e^{\pm i\varphi}}{r_0 \sin\theta} L_z,$$

which are obtained from the  $P_{\pm}$  operator by averaging with some harmonic oscillator function over  $(r - r_0)$ .

From the  $P_+J_- + P_-J_+$  operator we take for  $H_{\theta}$  the term

$$P^{(\theta)}_+J_- + P^{(\theta)}_-J_+$$

and from

$$P_+L_- + P_-L_+ + L_-P_+ + L_+P_- \quad (2.1)$$

we introduce into  $H_{\theta}$  those terms which remain after averaging of (2.1) over the  $(r - r_0)$  variable. These are the terms

$$(2/r_0)(\cos\theta L^2 + L^2 \cos\theta).$$

Thus the  $H_{\theta}$  operator for  $x \neq 0$  has the form

$$H_{\theta} = \left( \frac{\hat{x}^2}{8\mu_1 r_0^2} + \frac{1}{2\mu_2 r_0^2} \right) L^2 + \frac{1}{2\mu_1 R_0^2} [J^2 + L^2 - (2L_z^2 + L_+J_- + L_-J_+)] \\ - \frac{x}{8\mu_1 R_0} \left[ \frac{2}{r_0} (\cos\theta L^2 + L^2 \cos\theta) \right] + \frac{x}{4\mu_1 R_0} (P^{(\theta)}_+J_- + P^{(\theta)}_-J_+) + V(\theta).$$

## APPENDIX 3

We discuss here some other methods of solving the eigenvalue problem for bending-rotational and total Hamiltonians.

Let  $H_{\theta}$  be written in the form

$$H_{\theta} = H_{\text{rot}} + H_v + H_{rv},$$

with

$$H_{\text{rot}} = \frac{1}{2\mu_1 R_0^2} J^2, \\ H_v = \left( \frac{1}{2\mu_1 R_0^2} + \frac{1}{2\mu_2 r_0^2} \right) L^2 - \frac{1}{\mu_1 R_0^2} L_z^2 + V_{\theta}(\theta), \\ H_{rv} = - \frac{1}{2\mu_1 R_0^2} (L_+J_- + L_-J_+).$$

For every  $k$  we diagonalize  $H_v$  in the spherical function basis,  $Y_{lk}$ , and then with the help of the resulting functions

$$|L, k\rangle = \sum_l b_{lk} Y_{lk},$$

and the eigenfunctions for  $J^2$  we construct the basis for  $H_\theta$

$$(1/2^{\frac{3}{2}})(D^{J_{k0}}|L, k\rangle \pm D^{J_{-k0}}|L, -k\rangle), \quad D^{J_{00}}|L, 0\rangle.$$

This procedure permits us to obtain results up to high  $J$  values.

Another method of finding the eigenvalues of Hamiltonian (5) may also be proposed by analogy with the Bunker–Stone work. It includes the subdivision of the Hamiltonian (5) in the following way:

$$H = H_{\text{rot}} + H'_v + H_{rv},$$

$$H'_v = -\frac{1}{2\mu_2} \Delta_{\bar{r}} + \frac{1}{2\mu_1 R^2_0} (L^2 - 2L^2_z) + V(r, \theta).$$

Operator  $H'_v$  commutes with  $L_z$ , so that its eigenfunctions may be denoted as  $|L', k, N\rangle$ . The operator  $H'_v$  may be diagonalized in the basis of eigenfunctions of the operators  $H_v$  and  $H_r$ . The total Hamiltonian  $H$  must then be diagonalized in the basis

$$(1/2^{\frac{3}{2}})(D^{J_{k0}}|L', k, N\rangle \pm D^{J_{-k0}}|L', -k, N\rangle),$$

$$D^{J_{00}}|L', 0, N\rangle,$$

$$|L', k, N\rangle = \sum_{l,n} b^{L'kN}_{ln} Y_{lk} R_n,$$

$$|L', -k, N\rangle = \sum_{l,n} b^{L'kN}_{ln} Y_{l-k} R_n,$$

where the  $R_n(r)$  are chosen to be, for example, the eigenfunctions of a harmonic oscillator centered at  $r_0$ . From the computational point of view all previous attempts were only intended for decreasing the order of the secular equation.

The total operator may also be diagonalized in the basis composed of the products of the initial basis functions. The matrix obtained would have many zero elements (especially in the case of  $x = 0$ ). There exist some methods for diagonalization of such matrices. The most simple and suitable is Lanczos's method (28).

The effective bending–rotation Hamiltonian may be constructed directly from the operator (3). In such a case instead of  $H_\theta$  we would have

$$\tilde{H}_\theta = (1/2\mu_1 R^2_0)L^2_{\bar{R}} + (1/2\mu_2 r^2_0)L^2_{\bar{r}} + V(\theta).$$

The basis of bipolar spherical harmonics is appropriate for the diagonalization of this operator.

$$\{Y_{l_1}(\theta_1\varphi_1) \otimes Y_{l_2}(\theta_2\varphi_2)\} = \sum_{m_1 m_2} C^{JM}_{l_1 m_1 l_2 m_2} Y_{l_1 m_1} Y_{l_2 m_2}.$$

Here the  $C^{JM}_{l_1 m_1 l_2 m_2}$  are angular momentum coupling coefficients. The implicit integration over external variables may be performed in this case by analogy with the Back-



nell-Handy-Boys procedure (29). This scheme is very similar to the Le Roy-Van Kranendonk method (22). But to our mind calculations would be more practical with the Hamiltonian transformed to body-fixed axes.

The finite difference method may as well be applied to finding the eigenvalues and eigenfunctions of  $H_r$  and  $H_\theta$ . This method is very useful in solving the one-dimensional problem. In such a case the analogy of our work with that of Bunker-Stone (4) would be more complete.

#### APPENDIX 4

Let us discuss now the influence of the basis set. For  $J = 0$  we have basically the two-dimensional anharmonic oscillator for low-lying levels. The corresponding levels are found by  $H_\theta$  diagonalization in the free-rotator basis. The basis used is good for high levels but it is not appropriate for low-lying ones. So it is clear that a rather extended basis is needed and it yields a good estimate for a number of states at the same time. At  $k_\theta = 5.5 \times 10^{-3}$ ,  $k_\theta/\bar{B} = 500$ . So more than  $l_{\max}$  functions are needed to obtain the number of solutions which is more than the number of levels below the barrier,

$$l_{\max}(l_{\max} + 1) > k_\theta/\bar{B}, \quad \bar{B} = (1/2\mu_1 R^2) + (1/2\mu_2 r^2),$$

and

$$l_{\max} \geq (k_\theta/\bar{B})^{1/2}.$$

For  $k_\theta/\bar{B} \sim 500$  we have  $l_{\max} \sim 22$ -23. This is crude estimation for the basis size. The good approximation for all levels below the barrier may be achieved only with some larger basis.

The diagonalization of  $H_\theta$  with  $J = 0$  was performed using a basis composed of 50 and 80 functions, respectively. All 11 digits were the same in these two calculations for levels up to  $L = 35$ . The difference in the  $L = 42$  levels is about  $0.2 \text{ cm}^{-1}$  and a sharp difference begins only from  $L = 43$ . This shows that using 50 functions is sufficient for the estimation of  $\sim 40$  levels for  $J = 0$ .

Compare now two model calculations for  $J = 1^+$  with the basis of the form

$$D^l_{10} Y_{l1} + D^l_{-10} Y_{l-1}, \quad D^l_{00} Y_{l0}.$$

The basis size is  $N = 49$  ( $l_{\max} = 25$ ) and  $N = 79$  ( $l_{\max} = 40$ ). The energy difference exists even for  $L = 0$  level but it is negligible. For higher levels the differences are:  $L = 5 - 3 \times 10^{-6}$ ;  $L = 11 - 5 \times 10^{-3}$ ;  $L = 17 - 1.6$ ;  $L = 23 - 20 \text{ cm}^{-1}$ . The  $L = 23$  level is situated at  $\frac{3}{4}$  of the barrier height. So for the same basis size the accuracy decreases as the  $J$  value increases. The following practical rule may be stated. The basis composed of  $l_{\max} \approx (k_\theta/\bar{B})^{1/2}$  functions are to be used to obtain the levels below the barrier.

#### ACKNOWLEDGMENTS

The authors express their thanks to Professor N. G. Rambidi for stimulating interest in this work. We are very grateful to Professors A. Dymanus, T. Topping, Dr. P. Kuijpers, and to Dr. P. R. Bunker for making it possible for us to use their results prior to publication. Many thanks to Professors J. K. G. Watson, D. Papoušek, and Dr. V. Špirko for valuable comments and improving the manuscript.

RECEIVED: January 6, 1977

## REFERENCES

1. W. R. THORSON AND I. NAKAGAWA, *J. Chem. Phys.* **33**, 994 (1960).
2. K. F. FREED AND J. R. LOMBARDI, *J. Chem. Phys.* **45**, 591 (1966).
3. J. T. HOUGEN, P. R. BUNKER, AND J. W. C. JOHNS, *J. Mol. Spectrosc.* **34**, 136 (1970).
4. P. R. BUNKER AND J. M. R. STONE, *J. Mol. Spectrosc.* **41**, 310 (1972).
5. A. R. HOY AND P. R. BUNKER, *J. Mol. Spectrosc.* **52**, 439 (1974).
6. C. F. HANSEN, B. J. HENDERSON, AND W. E. PEARSON, *J. Chem. Phys.* **60**, 754 (1974).
7. D. PAPOUŠEK, J. M. R. STONE, AND V. ŠPIRKO, *J. Mol. Spectrosc.* **48**, 17, 38 (1973).
8. J. C. D. BRAND AND CH. V. S. RAMACHANDRA RAO, *J. Mol. Spectrosc.* **61**, 360 (1976).
9. J. M. R. STONE, *J. Mol. Spectrosc.* **54**, 1 (1975).
10. V. DANIELIS, D. PAPOUŠEK, C. ŠPIRKO, AND M. J. HORAK, *J. Mol. Spectrosc.* **54**, 339 (1975).
11. P. RUSSEGER AND J. BRICKMAN, *J. Chem. Phys.* **62**, 1086 (1975).
12. G. E. EWING, *J. Can. Phys.* **54**, 487 (1976), and references therein.
13. P. R. BUNKER, in "Vibrational Spectra and Structure" (J. R. Durig, Ed.), Vol. 3, Marcel Dekker, New York, 1975.
14. N. M. RODDITAS, S. M. TOLMACHEV, V. V. UGAROV, AND N. G. RAMBIDI, *Zh. Strukt. Khim.* **15**, 693 (1974), in Russian.
15. N. G. RAMBIDI, *J. Mol. Struct.* **28**, 77, 89 (1975).
16. A. M. SHAPOVALOV, V. F. SHEVEL'KOV, AND A. A. MAL'TZEV, *Vestnik MGU Ser. Khim.* **16**, 153 (1975), in Russian.
17. A. I. DEMENT'EV AND D. KRACHT, *Chem. Phys. Lett.* **35**, 243 (1975).
18. B. BAK, E. CLEMENTI, AND R. N. KORTZEBORN, *J. Chem. Phys.* **52**, 764 (1970).
19. E. CLEMENTI, H. KISTENMACHER, AND H. POPKIE, *J. Chem. Phys.* **58**, 2460 (1973).
20. G. A. NATANZON AND M. N. ADAMOV, *Vestn. LGU N4*, 28 (1974); *N10*, 24 (1974), in Russian.
21. A. V. LIAPTZEV AND A. A. KISELEV, *Opt. Spectrosc.* **39**, 466 (1975), in Russian.
22. R. J. LE ROY AND J. VAN KRANENDONK, *J. Chem. Phys.* **61**, 4750 (1974).
23. G. HENDERSON AND G. E. EWING, *J. Chem. Phys.* **59**, 2280 (1973).
24. S. I. VINITZKII AND L. I. PONOMAREV, *Nucl. Phys.* **20**, 576 (1974), in Russian.
25. R. T. PACK AND J. O. HIRSCHFELDER, *J. Chem. Phys.* **49**, 4009 (1968).
26. N. F. STEPANOV AND B. I. ZHILINSKII, *J. Mol. Spectrosc.* **52**, 277 (1974).
27. G. SIMONS AND J. M. FINLAN, *Phys. Rev. Lett.* **33**, 131 (1974).
28. C. LANCZOS, *J. Res. Nat. Bur. Stand.* **45**, 255 (1950).
29. M. G. BACKNELL, N. C. HANDY, AND S. F. BOYS, *Mol. Phys.* **28**, 759 (1974).
30. Z. K. ISMAIL, R. H. HAUGE, AND J. L. MARGRAVE, *J. Chem. Phys.* **57**, 5137 (1972).
31. Z. K. ISMAIL, R. H. HAUGE, AND J. L. MARGRAVE, *J. Mol. Spectrosc.* **45**, 304 (1973).
32. P. KUIJPERS, T. TÖRRING, AND A. DYMANUS, *Chem. Phys. Lett.* **42**, 423 (1976).
33. H. H. NIELSEN, in "Encyclopedia of Physics," Vol. 37, pp. 1, 187, Springer-Verlag, Berlin, 1959.
34. J. T. HOUGEN, *J. Mol. Spectrosc.* **48**, 609 (1973).
35. J. T. HOUGEN, *J. Chem. Phys.* **36**, 519 (1962).
36. D. A. VARSHALOVICH, A. N. MOSCALEV, AND V. K. KHERSONSKII, "Quantum Theory of Angular Momentum," Nauka, Leningrad, 1975, in Russian